

Effects of the Heat Input in the Mechanical Integrity of the Welding Joints Welded by GMAW and LBW Process in Transformation Induced Plasticity Steel (TRIP) Used in the Automotive Industry.

Victor H. López Cortéz¹, Gladys Y. Pérez Medina¹, Felipe A. Reyes Valdéz¹, Hugo F. López¹,

¹Corporación Mexicana de Investigación en Materiales, Saltillo, Coahuila, México, vlopez@comimsa.com

Resumo

Neste trabalho, uma chapa de aço de alta resistência (AHSS - Advanced High Strength Steel) tipo TRIP (Transformation Induced Plasticity) empregado atualmente no setor automotivo foi soldado usando o processo de soldagem a arco com arame sólido sob proteção gasosa (GMAW) e soldagem com LASER de CO₂ (LBW). As propriedades mecânicas das amostras soldadas quanto a tração e microdureza foram determinadas e os resultados foram relacionados com as microestruturas apresentadas. Verificou-se que a solda com LBW chegou a valores reativamente altos de dureza na zona fundida (ZF), indicando que a microestrutura resultante foi predominantemente de martensita. Na zona termicamente afetadas (ZTA), encontrou-se uma mistura de fases de bainita e ferrita. Misturas de fases semelhantes foram encontrados na ZTA e na ZF das amostras feitas com o processo GMAW. A microestrutura apresentada não sofreu degradação mecânica quando as amostras foram testadas à tração com todas as fraturas ocorrendo no metal de base (MB). Em contraste, a maioria das amostras de tração soldadas usando LBW falharam por clivagem frágil na região adjacente a ZTA. Aparentemente, nesta região ocorreu uma têmpera devido à dissipação de calor no processo LBW promovendo o crescimento de carbonetos e uma microestrutura relativamente grosseira. Nenhum fragilização foi encontrada que pudesse ser associada com o desenvolvimento da martensita.

Palavras-chave: aços AHSS, aço TRIP, Soldagem com LASER CO₂, GMAW.

Abstract: *In this work an Advanced High Strength Steel (AHSS) sheet of the Transformation Induced Plasticity (TRIP) type currently employed in the automotive sector was welded using a Gas Metal Arc Welding (GMAW) and a CO₂ Laser Beam Welding (LBW) processes. The mechanical properties of welded tensile specimens including microhardness were determined and the results were related to the exhibited microstructures. It was found that LBW lead to relatively high hardness in the fusion zone (FZ) indicating that the resultant microstructure was predominantly martensite. In the Heat Affected Zone (HAZ), a mixture of phases consisting of bainite and ferrite was present. Similar phase mixtures were found in the HAZ and Fusion Zone (FZ) of the GMAW samples. The exhibited microstructure did not result in mechanical degradation when the GMAW specimens were tested in tension as all the fractures occurred in the BM. In contrast, the region adjacent to the HAZ of most tensile specimens welded using LBW failed by brittle cleavage. Apparently, in this region tempering effects due to heat dissipation in the LBW process promoted carbide growth and a relatively coarse microstructure. No embrittlement was found that could be associated with the development of martensite.*

Key-words: AHSS steels; TRIP steel; LBW CO₂ welding; GMAW; Heat input.

1. Introduction

Due to high demand for energy saving, safety and emission reduction, Transformation induced plasticity steels (TRIP) have become very attractive materials for automotive industry. Welding of TRIP steels are one of the technical challenges in the successful application of AHSS in chassis structures, especially when the performance of the welded structures is required. Fusion welding process like GMAW and laser are used in the automotive industry, for joining mild steels. TRIP steel; however, do not offer the same ease of welding, and process control welding parameters is more critical. The welding parameters window represents the range of acceptable process parameters, primarily control of heat inputs, to obtain an acceptable weld. As a result, the effects of the heat input variations are greater

and TRIP steel has a narrower welding parameters window in which acceptable welds can be made. GMAW and Laser welding process for weld joints of this steel were used in order to obtain different heat inputs. Among the AHSS considered for applications in the automotive sector are transformation induced plasticity (TRIP) steels [1].

TRIP steels possess a microstructure consisting of ferrite and bainite including retained austenite. The steels exhibit relatively high work hardening rates and remarkable formability. The enhanced plastic behavior is attributed to the strain induced transformation of the retained austenite into martensite during the deformation process. In particular, the level of applied plastic strain needed to induce the austenite to martensite transformation is strongly dependent on the carbon content. At low carbon levels, the retained austenite transforms almost immediately once the material reaches the yield strength. At elevated carbon contents, the retained austenite becomes increasingly stable and can only transform at elevated levels of plastic straining such as the ones found during a sudden crash event [2].

Effects of the microstructural changes due to heat input

(Recebido em 12/03/2010; Texto final em 10/09/2010).

Table 1 Chemical composition of the AHSS TRIP 800.

Wt%	C	Mn	Si	P	Al	Cu	Cr	Ni	Mo	Sn
TRIP800	0.232	1.653	1.55	0.010	0.041	0.033	0.033	0.036	0.018	0.006

Table 2 Mechanical properties of the AHSS TRIP 800

Base Metal	Yield Strength [MPa]	Ultimate Tensile Strength [MPa]	Elongation [%]
TRIP800	450	800	28

Table 3 Welding Parameters and average microhardness using GMAW and CO₂ LBW processes in a TRIP800 steel

Welding Process	Joint type	Current [A]	Voltage [V]	Power [W]	Welding speed [m s ⁻¹]	Heat Input [J m ⁻¹]	Microhardness Average [Hv] HAZ
GMAW	Butt Joint	136	13	—	0.01333076	132,600	482.33
LBW CO ₂	Butt Joint	—	—	4,500	0.06166273	72,972.83	505.6

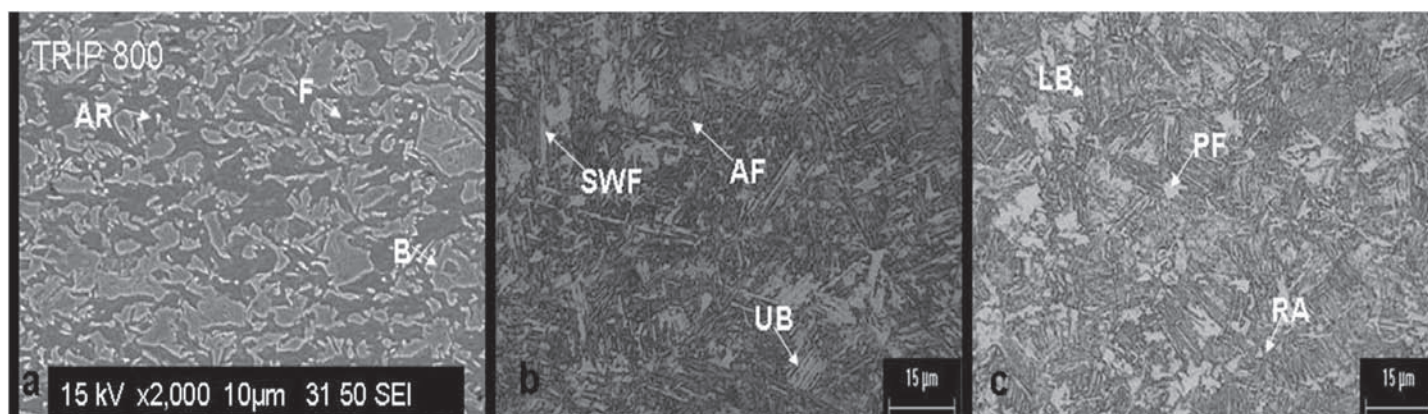


Figure 1. GMAW microstructures of the AHSS TRIP800 in (a) BM, (b) FZ and (c) HAZ.

applied can be detrimental for the mechanical integrity and the performance of the welding joints of these steels. Thus, it is important to determine the effect of welding on the resultant microstructures and on the exhibited mechanical properties obtained with different heat inputs. Among the main concerns related to welding is the formation of unwanted martensite [3, 4]. It has been found that in low heat input welding processes such as resistance spot welding, high carbon martensites can form in the weld that lead to embrittlement [3, 4]. Accordingly, in this work the effect welding on the resultant microstructures and on the mechanical integrity of a TRIP steel were investigated using a low and a high heat input processes. For this purpose, a gas metal arc welding (GMAW) and a Laser CO₂ welding processes were employed in welding a TRIP thin sheet steel currently used in the automotive sector.

2. Methods and Materials

Table 1 gives the chemical composition of the TRIP steel used in this work. The TRIP800 steel was supplied by the Italian

Institute Welding (IIW). Table 2 shows the mechanical properties of the TRIP steel in the form of 1.6 mm thick sheet. Tensile bars were cut from the steel sheet, each of size 244 x 70 x 1.6 mm and welded by GMAW and Laser CO₂ processes. The welding parameters used in the GMAW and Laser CO₂ processes are given in Table 3. In the case of the GMAW, the filler metal was of the type ER110S-G with a 1.6 mm diameter suitable for 780 MPa high tensile strength steels. The welding equipment employed was a Robot COMAU, CG4, RCC1, 17900582. In laser welding the equipment used was a CO₂-LBW-unit, EL.EN-RTM of 6 kW with 6 degrees of freedom. The exhibited microstructures and fracture modes of the Welded TRIP steels were characterized by metallographic means including optical and scanning electron microscopy (SEM). The exhibited hardness of the various welding regions was determined using a Vickers micro-hardness tester. In addition, the tensile strength and ductility of the welded strips was determined using a universal tensile testing machine.

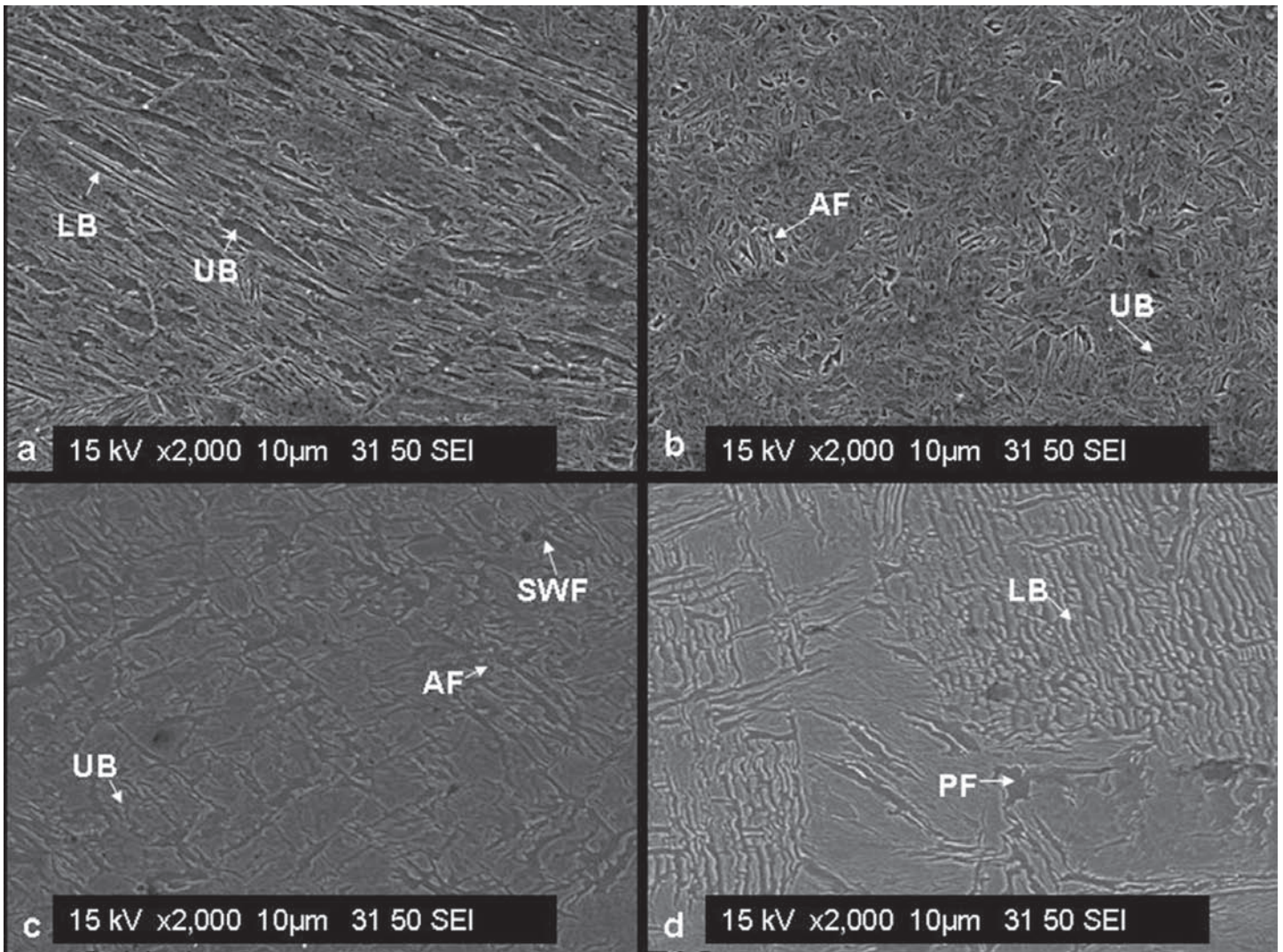


Figure 2. SEM micrographs of Laser CO₂ welding for (a) FZ and (b) HAZ and of GMAW for (c) FZ and (d) HAZ. Lower and upper bainite (LB, UB), allotriomorphic ferrite (AF), secondary widmanstatten ferrite (SWF), polygonal ferrite (PF).

3. Results and Discussion

3.1. Welded Microstructures

The microstructural features of the TRIP steel in the as received condition are shown in Figure 1a. Notice the mixture of ferrite and bainite and what seems to be some residual austenite. The resultant microstructures in the fusion zone (FZ) and Heat Affected Zone (HAZ) of the welded TRIP800 steel are shown in Figure 1b and 1c respectively. Notice from these micrographs that the exhibited microstructures in the steel welded using GMAW process were Secondary Widmanstatten Ferrite (SWF), Allotriomorphic Ferrite (AF) and Upper Bainite (UB) in the Fusion Zone (FZ). The HAZ contained Lower Bainite (LB), Polygonal Ferrite (PF) and possibly Retained Austenite (RA), as shown in figure 1c. In contrast, the fusion zone of the laser welded specimens shows what seems to be a fully martensitic structure as no evidence of ferrite or retained austenite could be found.

Figure 2 are SEM micrographs of the exhibited microstructures in the HAZ and the FZ for the laser and the GMAW processes. Notice from these figures that the amount of ferrite is significantly reduced in the FZ and it almost disappears in the HAZ when laser welding is used. The resultant microstructures in this case are mostly upper and lower bainite. In contrast, when GMAW is employed the resultant microstructures in the FZ and HAZ contain significant amounts of ferrite and possible austenite.

It is important to have a better understanding of the effect of the heat input in the microstructure changes, the knowledge of the amount of the heat and the cooling rate that was introduced in the weld joint due the welding process used in the present study. For this reason an estimation of the cooling rates exhibited by the weld metal was calculated using the following equation (1) [5]:

$$\frac{\partial \Theta}{\partial t} = - \frac{2\pi k_s^2}{\alpha} \left(\frac{v \Delta x}{Q \cdot} \right)^2 (\Theta - \Theta_o)^3 \quad (1)$$

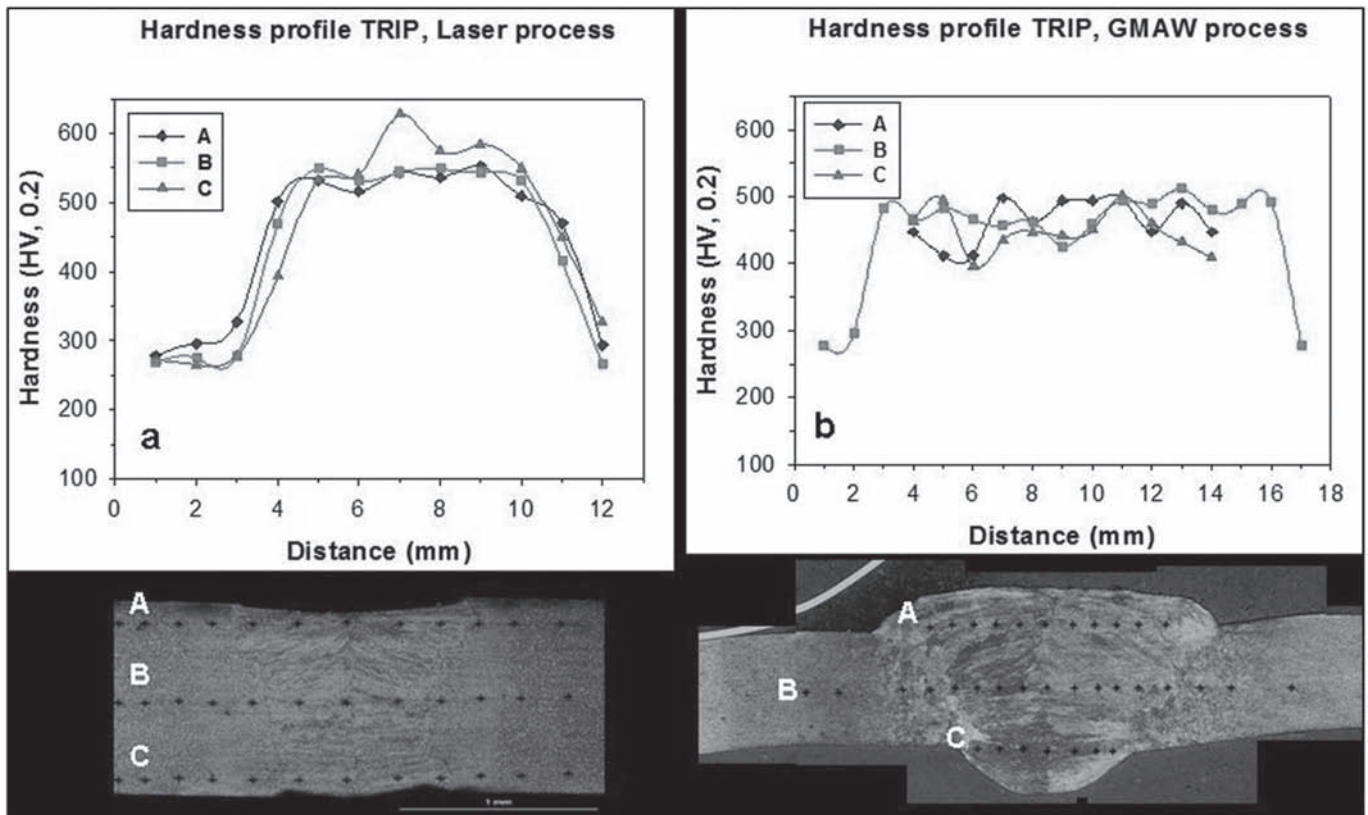


Figure 3. Exhibited microhardness profiles in the various regions of the welded TRIP800 using (a) Laser CO₂ welding and (b) GMAW.

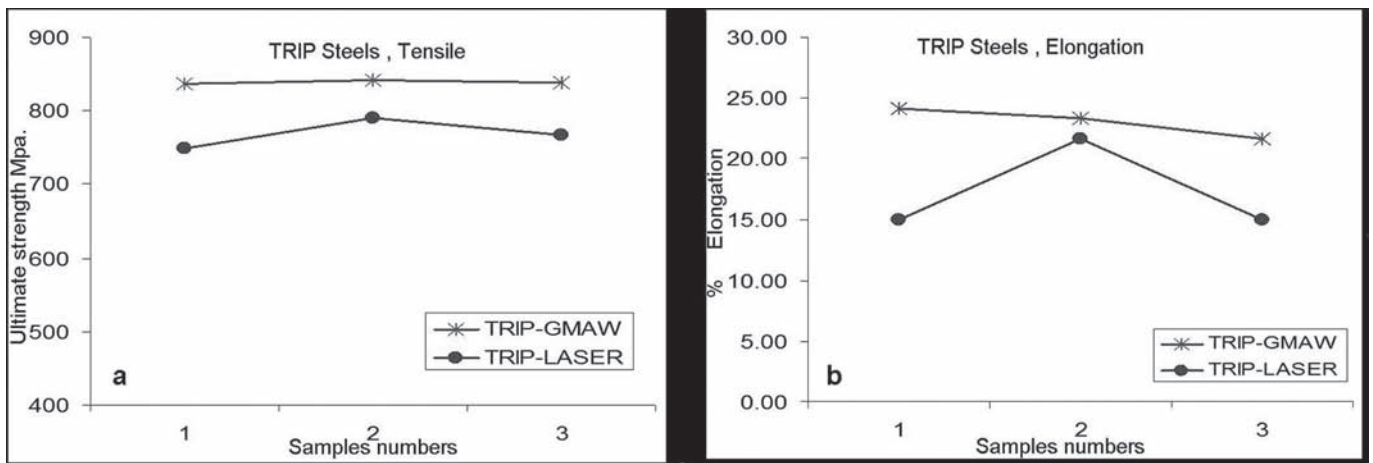


Figure 4. (a) Tensile strength of Laser CO₂ and GMAW welded TRIP800 steels and (b) corresponding weld elongations.

Where Q is the welding temperature (K), t time in seconds, k_s is the thermal conductivity of the steel, a is the thermal diffusivity in m^2s^{-1} , v is the welding speed (ms^{-1}), Q is the power input and Q_0 is the room temperature (K). From these estimations, cooling rates of the order of $144.67 Ks^{-1}$ were estimated for GMAW and of $417.81 Ks^{-1}$ for Laser CO₂ welding. From these results, it is clear that laser welding gives rise to relatively fast cooling rates. Critical cooling rates for the transformation of austenite (g) to martensite can be determined from continuous cooling transformation (CCT) diagrams. However, there are no reports on the continuous cooling transformation (CCT) curves for the

TRIP800 steel. Nevertheless, Bhadeshia [5] and Li [6] have proposed thermodynamically and kinetically based models for predicting CCT diagrams in a wide range of steels. From these estimations, it is found that in the present steel the critical cooling rates for the formation of martensite are between 45 and $90 Ks^{-1}$. Moreover, from the work of Gould et al [7], martensitic structures in the weld regions are likely to form at cooling rates above $90 Ks^{-1}$ in TRIP800 steels. Thus, embrittlement in the FZ can be a potential problem in these steels, particularly when Laser CO₂ welding is employed.

Since the heat input during welding using the GMAW

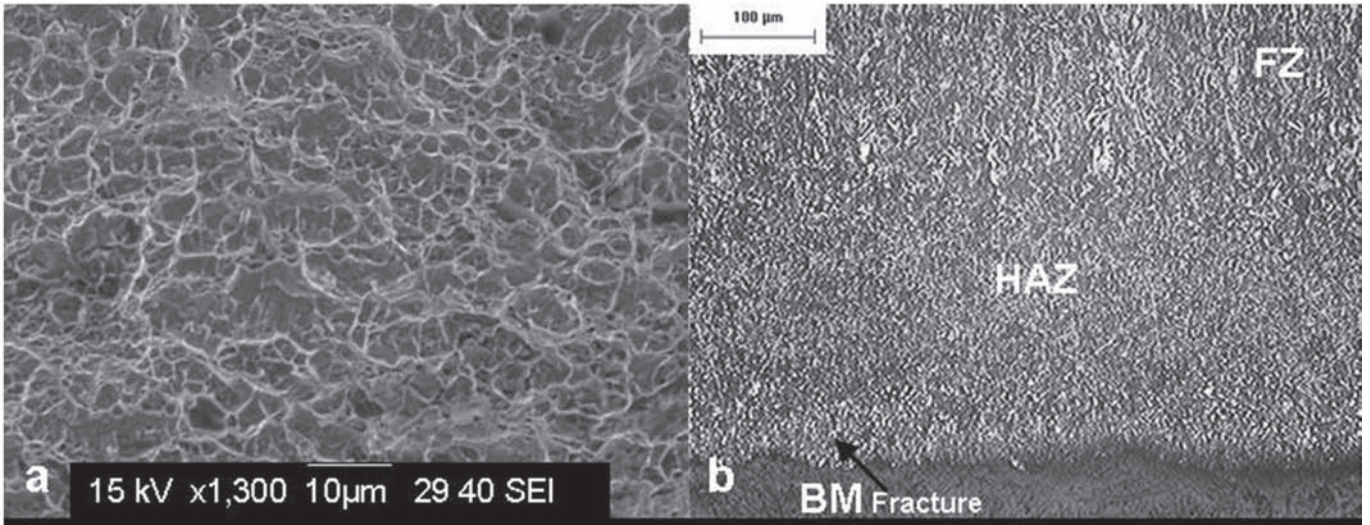


Figure 5. (a) SEM micrograph showing the ductile fracture appearance of the BM consisting of a typical dimple fracture rupture and (b) optical micrograph showing the fracture location in a Laser CO₂ welded strip.

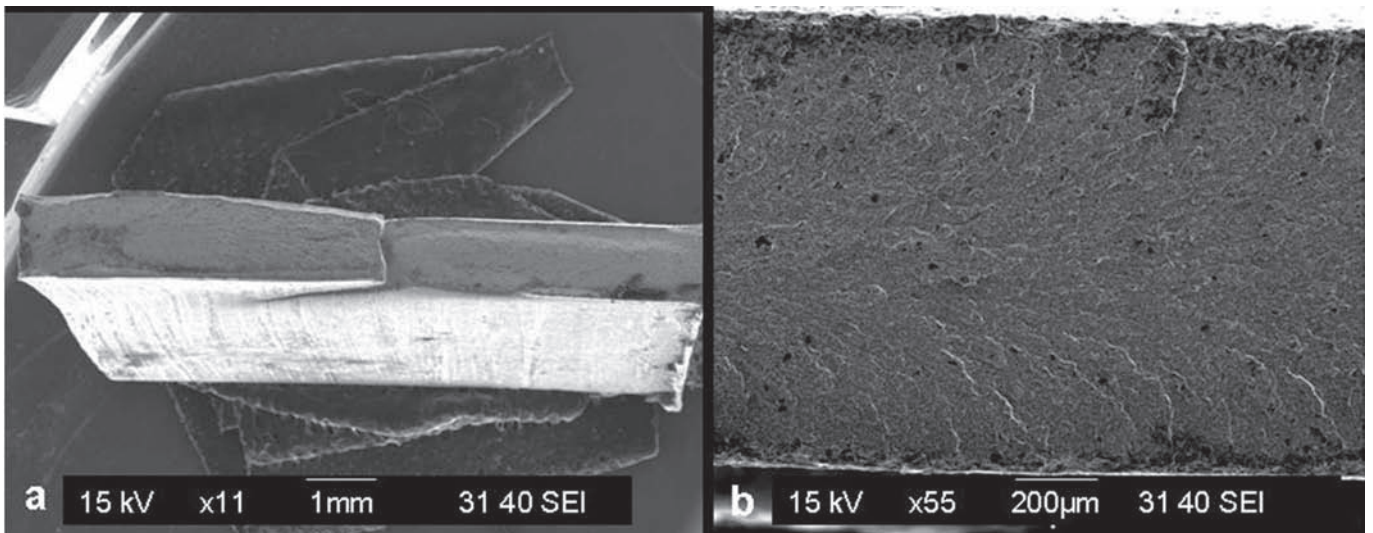


Figure 6. Overall view of the fracture surfaces; (b) brittle fracture appearance typical of cleavage with what seemed to be river markings.

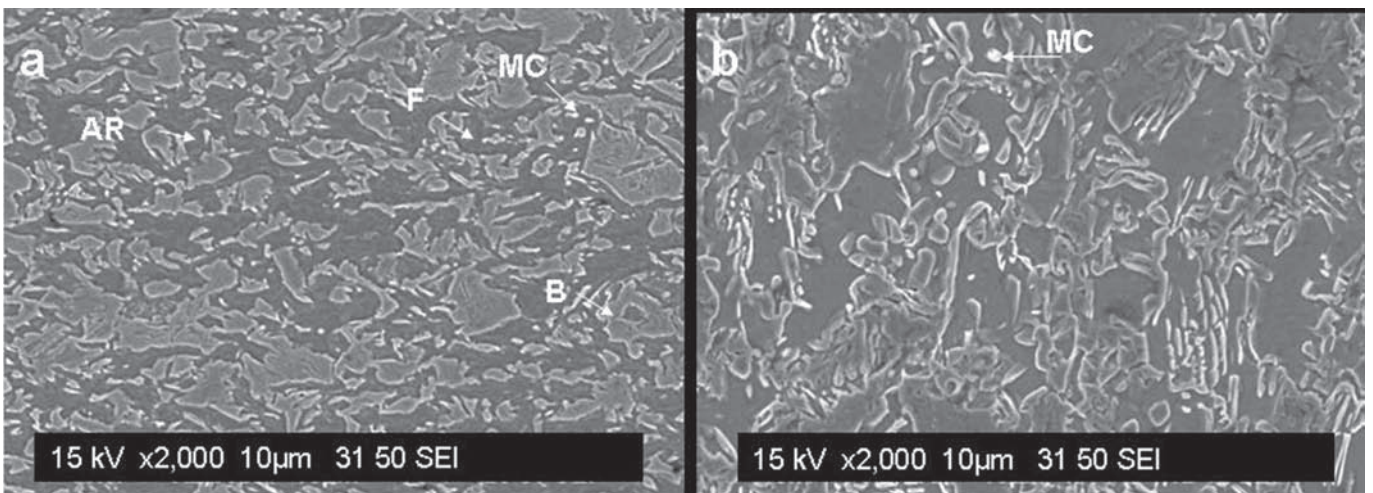


Figure 7. A comparison of the resultant microstructures in the BM region of the Laser CO₂ process. (a) BM region adjacent to the HAZ and (b) BM region away from the HAZ.

process is almost twice the heat input of the laser process (see Table 3), the exhibited cooling rates are significantly reduced in this case. In turn, the resultant microstructures in both, the FZ and HAZ consist of a mixture of ferrite, bainite, martensite and possible retained austenite (see Figure 2).

In addition, the introduction of residual stresses in the HAZ particularly in Laser CO₂ welding can be a major concern as the thermal cycle is relatively fast. Thermal stresses can lead to strain induced martensite (SIM) transformation from the retained austenite. In turn, this would result in an increase in hardness but lower ductility in the HAZ including the HAZ-BM neighborhood, as well as to the development of internal stresses in these regions.

3.2. Microhardness

Figures 3a and 3b show the microhardness profiles for the various regions of the welded TRIP800 using the two welding processes. The numbers represents the locations of indentations at 1 mm spacing. Notice that in the laser welded TRIP800 steel the average microhardness increases from 275 HV in the BM to up to 500 HV in the HAZ and over 600 HV in the FZ. In particular, the microhardness profiles resemble a “top hat” morphology [7] with a maximum hardness of 600 HV in the parting line. These microhardness profiles are attributed to the development of athermal martensite [7] which no longer depends on the cooling rates. In the GMAW, the microhardness profiles did not follow the same trends as in the Laser CO₂ welding process. In this case, the actual cooling rates were not high enough to avoid the development of a mixture of phases (ferrite, bainite and martensite) in the FZ and HAZ regions. In this case, maximum Vickers hardness values of up to 500 HV were found in the welded regions.

From the microhardness measurements it is clear that welding leads to a significant increase in hardness in the welded regions. In particular, it is found that the metal in the regions adjacent to the HAZ of the laser welded strips exhibited a significant increase in hardness (points 4 and 11 in Figure 3a). This effect was not observed when GMAW was employed. Apparently, due to the relatively high cooling rates, possible SIM and the development of residual stresses might have occurred in the BM region adjacent to the HAZ as there were no clear phase transitions identified in this region.

3.3 Tensile strength.

Figures 4a and 4b show the tensile strength (UTS) and ductility exhibited by the welded TRIP800 steels. Notice from this figure that both, UTS and % elongation drop in the laser welded strips when compared with the GMAW ones. In the laser welded specimens the maximum UTS values did not reach 800 MPa in contrast with the ones welded using GMAW (see Figure 4a). Also, the elongation of the laser welded TRIP steels drops down to 15 % or below when compared with the elongation of GMAW which exhibit elongations in the range of 25 %. In turn, this clearly indicated that laser welding of TRIP800 steels leads to a reduction in the steel toughness when compared with the

GMAW process.

Confirmation for the loss of toughness was found by looking at the fracture regions (see Figure 5). It was found that in the specimens welded using GMAW the fracture location was always in the BM away from the welded regions. The fracture surfaces were typical of a ductile material with numerous dimples and appreciable plastic deformation (see Figure 5a). In turn this indicated that the mechanical strength of the GMAW welded regions was superior to the strength of the BM. In contrast, in the laser welded steels, fracture occurred in the BM regions adjacent to the HAZ as shown in Figure 5b. Also, the fracture appearance was brittle cleavage with what seemed to be river markings (see Figures 6a-b). Notice the lack of enough ductility as the fracture surfaces were relatively flat and there was a lack of appreciable cavitation.

Although, in the BM adjacent to the HAZ the microstructure is typical of a ferritic matrix with bainite and possible retained austenite, it seems that this region becomes susceptible to fracture as a result of (a) SIM driven by internal stressing and (b) the development of possible residual/internal stresses at this location as a result of the fast cooling rates exhibited. Evidence for an increase in hardness in this location is found by the microhardness measurements. Notice from figure 3a that in the BM region adjacent to the HAZ hardness values increase appreciably when compared with the BM away from the HAZ.

The hardness increases in the BM region adjacent to the HAZ can only be accounted for through the development of internal stresses and/or the formation of martensite from any residual austenite. A comparison of the resultant microstructures in the BM region adjacent to the HAZ with the one away from the HAZ is given in Figure 7. Notice from these figures that appreciable coarsening of the various phase constituents occurs in the BM adjacent to the HAZ. Moreover, precipitation and/or growth of what seems to be carbide phases (see Figure 8) is also active in this region. Accordingly, it is apparent that in the HAZ of the Laser CO₂ welded strips tempering effects coupled with phase coarsening and residual stresses including SIM promote brittleness. This effect is not observed in the GMAW process indicating that the magnitude of residual stresses developed in the BM regions adjacent to the HAZ is not high enough to induce brittleness.

Finally, the potential for martensite embrittlement at the parting line of the FZ when low heat input welding processes such as Laser CO₂ is employed was not supported by the experimental outcome of this work. Even though, the TRIP 800 steel welded by these means underwent a loss of toughness, the effect could not be linked to the presence of unwanted martensite in the FZ. Laser welding is known to give rise to minimal microstructural damage as the FZ and HAZ are relatively narrow. The outcome of this work indicates that the potential for martensite embrittlement might not occur by Laser welding, yet, additional work is needed to identify welding parameters which will avoid the loss of strength and ductility such as the one found in the BM regions near the HAZ.

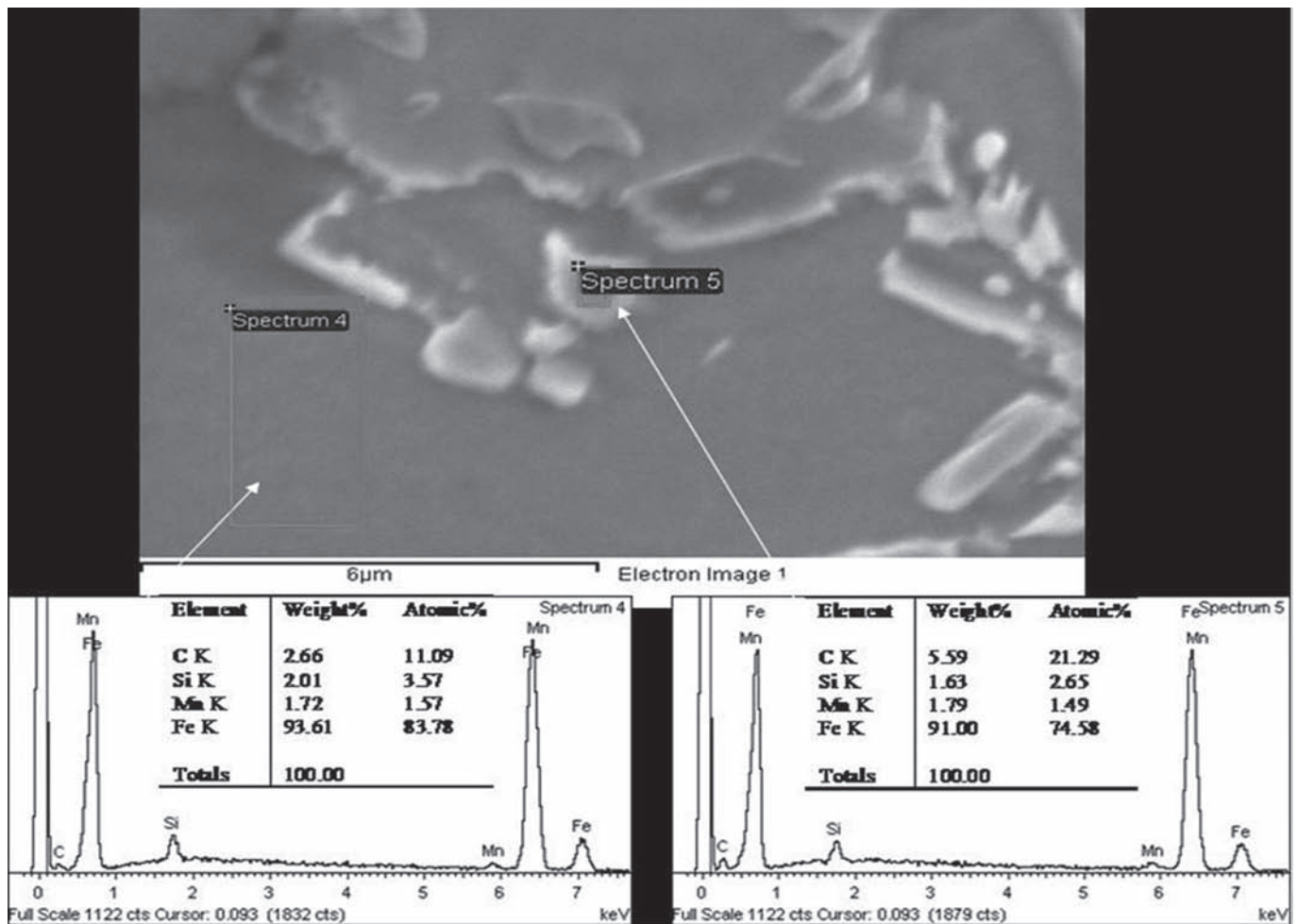


Figure 8. SEM micrograph of what seems to be a carbide phase including EDX composition spectra.

4. Conclusions

Microhardness measurements were combined with tensile testing in investigating the weldability of a thin sheet of a TRIP 800 steel using GMAW and Laser CO₂ processes. It was found that:

1. Welding using Laser CO₂ resulted in fully martensitic structures in the fusion zone and a mixture of bainite and ferrite in the HAZ.
2. The FZ including the HAZ were relatively hard compared with the BM.
3. GMAW promoted the development of mixtures of predominantly bainite and ferrite phases in both the FZ and HAZ,
4. The measured mechanical properties indicated that in samples welded using Laser CO₂, the BM region adjacent to the HAZ underwent brittle fracture. Apparently, tempering of the phases in this region resulted in weakening through phase coarsening and carbide precipitation/growth.
5. In both welding processes, no embrittlement could be found that can be attributed to the formation of martensite.

5. Acknowledgments

Thanks for Financials support from Consejo Estatal de Ciencia y Tecnología from Coahuila State, México.

6. References

1. BY N. Kapustka. C. Conrardy, S. Babu. 'Effect of GMAW process and Material Conditions on DP 780 and TRIP 780 Welds', *Welding Journal* 2008.
2. I.D.Choi et al. 'Deformation behaviour of low carbon TRIP sheet steels at high strain rates'. *ISIJ Int* 2002; 42(12):1483–9; 2002.
3. J. E., Gould, L. R. Lehman, S. Holmes. 'A design of experiments evaluation of factors affecting the resistance spot weldability of high-strength steels'. *Proc. Sheet Metal Welding Conference VII, AWS Detroit Section*, 1996.
4. J. E., Gould, D. Workman, 'Fracture morphologies of resistance spot welds exhibiting hold time sensitivity behavior'. *Proc. Sheet Metal Welding Conference VIII, AWS Detroit Section*. 1998.
5. Bhadeshia, H. K. D. H; and Svensson, L-E 1993. *Mathematical Modeling of Weld Phenomena*, eds, H. Cerjack and K. E. Easterling, Institute of Metals, London, pp.109-180.

6. Li, M. V; Niebuhr, D. V; Meekisho, LL and Atteridge, D.G.1998. 'A computational model for the prediction of steel hardenability'. Metallurgical and Materials Transactions 29B (6):661-672.
7. J.E. Gould, S.P. Khurana, T. Li; 'Predictions of microstructures when welding automotive advanced high-strength steels'; *Welding Journal*, AWS, May 2006, 111.